Coupling of Gaussian Beam and Finite Difference Solvers for Semiclassical Schrödinger Equations

Emil Kieri[1,*], Gunilla Kreiss[1] and Olof Runborg[2]

[1] *Division of Scientific Computing, Department of Information Technology, Uppsala University, Sweden*
[2] *Department of Mathematics and Swedish e-Science Research Center (SeRC), KTH, Sweden*

Abstract. In the semiclassical regime, solutions to the time-dependent Schrödinger equation for molecular dynamics are highly oscillatory. The number of grid points required for resolving the oscillations may become very large even for simple model problems, making solution on a grid intractable. Asymptotic methods like Gaussian beams can resolve the oscillations with little effort and yield good approximations when the atomic nuclei are heavy and the potential is smooth. However, when the potential has variations on a small length-scale, quantum phenomena become important. Then asymptotic methods are less accurate. The two classes of methods perform well in different parameter regimes. This opens for hybrid methods, using Gaussian beams where we can and finite differences where we have to. We propose a new method for treating the coupling between the finite difference method and Gaussian beams. The new method reduces the needed amount of overlap regions considerably compared to previous methods, which improves the efficiency.

1 Introduction

We consider the dynamics of atomic nuclei, which is decoupled from the electron dynamics through the Born–Oppenheimer approximation [30]. The atoms may be part of a single molecule, or of the reactants and products of a chemical reaction. Our model is the

*Corresponding author.
Email: emil.kieri@it.uu.se (E. Kieri), gunilla.kreiss@it.uu.se (G. Kreiss), olofr@nada.kth.se (O. Runborg)

time-dependent Schrödinger equation (TDSE) in semiclassical scaling,

$$i\varepsilon u_t = -\frac{\varepsilon^2}{2}\Delta u + Vu, \quad x \in \mathbb{R}^n, \quad t > 0, \tag{1.1a}$$

$$u(x,0) = u_0(x). \tag{1.1b}$$

The wave function $u = u(x,t)$ contains all retrievable information about the system. In particular, the squared modulus $|u(x,t)|^2$ is the probability density of the nuclei being located at the coordinates x at time t. The probability distribution for other properties, such as momentum and energy, can be extracted by applying operators to the wave function. The Hamiltonian $-(\varepsilon^2/2)\Delta + V$ is the operator for the total energy of the molecular system, and its two terms correspond to the kinetic and potential energies, respectively. The scaling parameter ε is the reciprocal square root of some characteristic mass for the problem. For heavier particles, and thus smaller ε, the problem behaves more classically. The limit $\varepsilon \to 0$ is called the semiclassical limit. The range of interesting ε is between 1 and 10^{-3}, corresponding to the masses of an electron and an uranium atom, respectively. In this paper we focus on semiclassical problems, i.e., problems with heavy particles. Such problems typically feature wave packets of width $\mathcal{O}(\sqrt{\varepsilon})$ and with wavelength $\mathcal{O}(\varepsilon)$, i.e., localised highly oscillatory solutions.

Solving highly oscillatory problems on a grid is often prohibitively expensive due to the vast number of grid points required for resolving the oscillations. This difficulty is not specific to the Schrödinger equation but common to all high frequency wave propagation problems. When resolving the oscillations on a grid becomes unfeasible one has to resort to something else, commonly asymptotic methods. Such methods have been studied in the fields of acoustics, seismology and electromagnetics [6, 15] as well as in quantum dynamics [13]. Asymptotic methods have modelling errors which are dependent on some problem parameter. For high frequency wave propagation problems the modelling error typically decays in the high frequency limit. This is the case for the method of Gaussian beams [1, 5, 27, 28], which we will consider in this work. A Gaussian beam is a complex-valued basis function with Gaussian profile which is propagated along a classical trajectory. Its phase exhibits oscillations with wave length of order ε, and if the potential V is a polynomial of at most second order Gaussian beams solve the TDSE exactly. By adding higher order terms to the amplitude and phase, higher order Gaussian beams can be constructed. Error estimates, in terms of the parameter ε, for more general potentials and Gaussian beams of arbitrary order were shown in [21]. In parallel to their development in the applied mathematics community, Gaussian beams were discovered by chemical physicists [8] motivated by the observation that if the potential is a quadratic polynomial, a Gaussian wave function will stay Gaussian for all time.

Gaussian beams perform well for short wave lengths, i.e., for small ε. The model assumption is that the features of the potential V have a length scale which is long compared to the width of a beam. In applications this is not always valid, the particle masses and the potential are problem parameters beyond our control. In this paper we focus on the situation where the potential is smooth and slowly varying in most of the domain,

but locally has features on a scale comparable to the wave length. This motivates the construction of a hybrid method which uses Gaussian beams where the potential is smooth, and direct solution on a grid in the vicinity of fine-scale features of the potential. Such a hybrid method was developed for the wave equation in [32], where abrupt changes in propagation speed give rise to the same difficulties as rapidly varying potentials. A hybrid method for the TDSE was developed in [14]. That method is robust and general, but it relies on rather extensive buffer regions for the translation between grid and Gaussian beam representations. One therefore has to use the more expensive grid method in a significantly larger part of the domain than the extension of the fine-scale features of the potential. Furthermore, one has to solve an optimisation problem each time a new Gaussian beam is spawned from the grid representation of the solution. We present a new, more efficient method for translation between the representations. In our method the buffer regions do not need to be thicker than around 30 grid points, independently of the resolution and of the parameter ε, and we do not have to solve any optimisation problems. The drawback of our approach is loss of generality, it is not applicable to any potential. The potential must not vary too fast near the edge of the grid in order to assert that the beams will not change directions while intersecting an interface.

The remainder of this paper is organised as follows. In Section 2 we describe the Gaussian beams and the finite difference method which are used for the spatial discretisation of the problem (1.1a)-(1.1b). We also describe the absorbing boundary conditions with which we close the finite difference domain. In Section 3 we describe how the methods are coupled, and prove an error estimate for the translation from grid representation to Gaussian beams. We describe how the spatially discretised solution is propagated in time in Section 4. In Section 5 we demonstrate the method with numerical examples in one and two dimensions. We also validate the error estimate from Section 3 numerically. Conclusions are drawn in Section 6.

2   Spatial discretisation

2.1   Gaussian beams

In this section we briefly review the construction of first order Gaussian beams. For a more thorough presentation, and generalisation to higher order beams, we refer to [13, 21].

A first order Gaussian beam in $\mathbb{R}^n$, parametrised by its initial centre coordinate y, is given by

$$v(x,t;y) = (2\pi\varepsilon)^{-n/2}a(t;y)e^{i\phi(x-q(t;y),t;y)/\varepsilon} \tag{2.1}$$

with the phase

$$\phi(\xi,t;y) = \phi_0(t;y) + \xi^T p(t;y) + \frac{1}{2}\xi^T M(t;y)\xi. \tag{2.2}$$

The imaginary part of the complex symmetric matrix M is positive definite, so that v

indeed is a Gaussian. The amplitude and phase variables of the beam are propagated according to the system of ordinary differential equations (ODEs)

$$\dot{a} = -\frac{1}{2}a\text{Tr}(M), \qquad\qquad \dot{q} = p, \tag{2.3a}$$

$$\dot{\phi}_0 = \frac{p^2}{2} - V(q), \qquad\qquad \dot{p} = -\nabla V(q), \tag{2.3b}$$

$$\dot{M} = -M^2 - \nabla^2 V(q). \tag{2.3c}$$

a and M are complex-valued, while ϕ_0, p and q are real. The gradient operator ∇ is a column vector, and $\nabla^2 f(y)$ denotes the Hessian matrix of $f(x)$ at $x = y$. If the initial condition (1.1b) to the TDSE can be represented by a Gaussian beam, $u(x,0) = v(x,0;y_0)$, the error at time $t \in [0,T]$ is bounded by

$$\|u(\cdot,t) - v(\cdot,t;y_0)\|_{L_2} \leq C_T\sqrt{\varepsilon}. \tag{2.4}$$

The constant C_T depends on T and on the potential, but is independent of ε. This result is proven in, e.g., [7]. A general initial condition can be approximated by an integral superposition of Gaussian beams, also then the propagation error is bounded by $C_T\varepsilon^{1/2}$ [21].

In [31, Theorem 2.1] it was shown how to approximate a smooth function by an integral superposition of Gaussian beams, and what error bounds such superpositions satisfy. The following theorem is a simplified statement of that result. We will use the notation

$$f(x) = T_p^y[f](x) + R_p^y[f](x) \tag{2.5}$$

for the pth order Taylor expansion of a function $f(x)$ around y, and its remainder.

Theorem 2.1 (Tanushev [31]). *Given a function*

$$u_0(x) = A_0(x)e^{i\Phi_0(x)/\varepsilon} \tag{2.6}$$

with $A_0 \in C_0^\infty(\mathbb{R}^n, \mathbb{C})$ and $\Phi_0 \in C^\infty(\mathbb{R}^n, \mathbb{R})$ independent of ε, and $\varepsilon > 0$, let the Gaussian beams

$$v(x;y) = \left(\frac{1}{2\pi\varepsilon}\right)^{n/2} A_0(y)\exp\left(\frac{i}{\varepsilon}T_2^y[\Phi_0](x) - \frac{1}{2\varepsilon}\|x-y\|^2\right). \tag{2.7}$$

Then the integral superposition of $v(\cdot;y)$ approximates u_0, and the error is bounded by

$$\left\|\int_{\mathbb{R}^n} v(\cdot;y)\mathrm{d}y - u_0\right\|_{L_2} \leq C\sqrt{\varepsilon}. \tag{2.8}$$

Guided by this result we can approximate general initial data u_0, decomposed in amplitude and phase, by an integral superposition of Gaussian beams with the initial variable values

$$a(0;y) = A(y), \qquad\qquad q(0;y) = y, \tag{2.9a}$$

$$\phi_0(0;y) = \Phi(y), \qquad\qquad p(0;y) = \nabla\Phi(y), \tag{2.9b}$$

$$M(0;y) = \nabla^2\Phi(y) + iI. \tag{2.9c}$$

In computations, the integral superposition has to be replaced by a finite sum. A spacing of order $\sqrt{\varepsilon}$ between the beams then suffices. This can be seen by investigating how a sum of shifted Gaussians approximate unity [9].

2.2 Finite difference operators

In the part of the domain where we solve the TDSE on a grid, we use high order finite difference operators on summation-by-parts (SBP) form [19, 20]. The reason for this choice is threefold. First, the TDSE is sensitive to dispersion errors, and the higher frequencies are more difficult to handle. Dispersion relations are captured more accurately by higher order methods. Second, the method we use to translate the solution from Gaussian beam to grid representation, which is described in Section 3.1, requires stencils of finite width. This disqualifies the Fourier pseudospectral method [17, 18], since it involves all available grid points. It is otherwise both accurate and efficient when solving the TDSE on a grid. Third, with SBP operators it is straight-forward to implement stable boundary conditions using a simultaneous approximation term (SAT) [4]. SBP-SAT discretisations can be shown to be energy-stable for several classes of initial-boundary value problems. Stable Dirichlet boundary conditions for the TDSE were derived in [26], and are summarised here.

Consider the TDSE on $0 \le x \le 1$ with homogeneous Dirichlet boundary conditions, and an inhomogeneous term $F(x,t)$ added to the right-hand side. We discretise the domain with an equidistant grid, which includes the boundary points. We denote grid functions, i.e., vectors containing function values on the grid points, with boldface letters. The spatially discretised problem then reads

$$i\varepsilon \dot{\mathbf{u}} = -\frac{\varepsilon^2}{2}D_2\mathbf{u} + V\mathbf{u} + \frac{\varepsilon^2}{2}P^{-1}S^T B\mathbf{u} + \mathbf{F}, \tag{2.10a}$$

$$\mathbf{u}(0) = \mathbf{f}, \tag{2.10b}$$

where D_2 is an SBP operator approximating the second derivative, S approximates the first derivatives at the boundaries, $B = \mathrm{diag}(1,0,\cdots,0,-1)$, and P is a diagonal positive definite matrix which defines the norm $\|\mathbf{u}\|_P = (\mathbf{u}^*P\mathbf{u})^{1/2}$. The elements of P are chosen in a special way, such that the discretisation satisfies an energy estimate, and we have $\|\mathbf{u}\|_P \approx \int_0^1 |u|^2 \mathrm{d}x$. The term $(\varepsilon^2/2)P^{-1}S^T B\mathbf{u}$ is the SAT, a penalty term which enforces the boundary conditions weakly. The boundary conditions are therefore not satisfied exactly, but have error of the same order as the error of the internal scheme. The semidiscretised equation (2.10) then satisfies the energy estimate

$$\|\mathbf{u}(t)\|_P \le \|\mathbf{f}\|_P + \frac{1}{\varepsilon}\int_0^t \|\mathbf{F}(\tau)\|_P \mathrm{d}\tau. \tag{2.11}$$

Details about the SBP operators and their derivation are given in [23].

2.3 Absorbing boundary conditions

Since there is no physical boundary around the finite difference domain we enclose it by non-reflecting boundary conditions, which are implemented using perfectly matched layers (PMLs) [2]. We use the modal PML presented in [25], which in one dimension is implemented by modifying the kinetic part of the Hamiltonian to

$$-\frac{\varepsilon^2}{2}\frac{1}{1+e^{i\gamma}\sigma(x)}\frac{\partial}{\partial x}\frac{1}{1+e^{i\gamma}\sigma(x)}\frac{\partial}{\partial x}. \tag{2.12}$$

At the right-hand side boundary we use the polynomial damping function

$$\sigma(x)=\begin{cases} \sigma_0\left(\dfrac{x-x_{\text{PML}}}{d}\right)^r, & x\geq x_{\text{PML}},\\ 0, & x<x_{\text{PML}}. \end{cases} \tag{2.13}$$

Such a layer absorbs outgoing waves efficiently and accurately. A similar damping function is used at the left-hand side boundary.

When using the PML, the second derivative appears with a variable coefficient. SBP operators for the second derivative with variable coefficients on the form $\frac{\partial}{\partial x}g(x)\frac{\partial}{\partial x}$ were derived in [16, 22]. These operators make the implementation of the PML straight-forward. Let $g(x)=(1+e^{i\gamma}\sigma(x))^{-1}$, $G=\text{diag}(g(x_j))$, and $B^{(g)}=\text{diag}(g(x_0),0,\cdots,0,-g(x_N))$. The SBP operator approximating $\frac{\partial}{\partial x}g(x)\frac{\partial}{\partial x}$ is then

$$D_2^{(g)}=P^{-1}(-M^{(g)}-B^{(g)}S), \tag{2.14}$$

where $M^{(g)}$ is complex symmetric. It has positive semidefinite real part and negative semidefinite imaginary part. The semidiscretised TDSE with PML then reads

$$i\varepsilon\dot{\mathbf{u}}=-\frac{\varepsilon^2}{2}GD_2^{(g)}\mathbf{u}+\frac{\varepsilon^2}{2}P^{-1}S^TB^{(g)*}G^*\mathbf{u}+V\mathbf{u}. \tag{2.15}$$

The outer boundaries of the PMLs still need to be closed with boundary conditions, but since the solution is effectively damped in the layer the choice of boundary conditions is not crucial. Above, we use homogeneous Dirichlet boundary conditions. This discretisation, as any other discretisation of the modal PML [25], has not been proven to be stable, but we do not experience any signs of numerical instabilities in our computations.

3 Coupling the methods

In this section we describe how we handle the coupling between the subdomains treated with finite differences and Gaussian beams. Fig. 1 illustrates how the domain is decomposed in one dimension, and where translation between the two representations happen. We solve the TDSE with finite differences between, and including, the shaded areas in
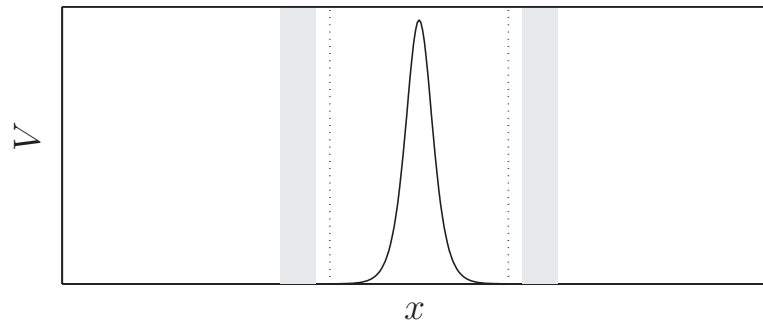
Figure 1: Sketch of how the domain is decomposed. The solid line shows the potential barrier which is responsible for the nontrivial scattering, and resides in the finite difference domain. The dotted lines denote the Huygens' surfaces, where Gaussian beams are transferred to grid representation. The PMLs reside in the shaded areas, and new beams are spawned in the region between the Huygens' surfaces and the PMLs.

Fig. 1. The region between the dotted lines is where we judge solution by finite difference necessary due to sharp variations in the potential. The rest of the finite difference domain is needed for coupling with the Gaussian beams. As representation of the wave function we take the finite difference solution between the dotted lines, and the Gaussian beams outside them.

We adopt the point of view of the finite difference domain, calling translation from Gaussian beams to grid representation inflow, and from grid representation to Gaussian beams outflow. The dotted lines in Fig. 1 constitute the inflow interfaces. These are implemented as Huygens' surfaces, and are described in more detail in Section 3.1. The outflow buffers, regions as wide as the difference stencil where new Gaussian beams are spawned, are located between the dotted lines and the shaded areas. We need them to be outside the inflow interfaces in order to prevent the inflow from disturbing the handling of the outflow. The outflow buffers are described in Section 3.2. The finite difference domain is enclosed by PMLs, which reside in the shaded areas.

3.1 Inflow to the grid

The inflow interfaces, marked by dotted lines in Fig. 1, are implemented using Huygens' surfaces. Huygens' surfaces allow us to put the interface in the interior of the grid. This is desirable since we want to handle the outflow closer to the boundary of the grid than the inflow interface. This would not have been possible if we had handled inflow with inhomogeneous boundary conditions. Huygens' surfaces are often used when scattering problems are solved in the field of electromagnetics, but little for other applications. The technique is carefully described for Maxwell's equations in [29, Chapter 6.5] under the name "total-field/scattered-field formulation". Application to the TDSE is analogous. The idea is to partition the solution in its incident and scattered parts,

$$u = u^{\text{inc}} + u^{\text{scat}}, \tag{3.1}$$

where u^{inc} is known. In our method, u^{inc} is the part of the solution treated with Gaussian beams. The grid is divided into two parts. In one part, where the nontrivial scattering happens, the total solution u is represented on the grid. This is in our case the region between the two Huygens' surfaces. Outside the Huygens' surfaces, where Gaussian beams are considered to be accurate enough, only u^{scat} is represented on the grid. This part of the grid is in our method the narrow outflow buffers, only wide enough to allow for translation of u^{scat} to Gaussian beam representation.

A Huygens' surface is implemented as follows. Consider the Cauchy problem with a Huygens' surface at $x = 0$. The solution put on the grid is

$$v(x,t) = \begin{cases} u^{\text{scat}}, & x < 0, \\ u^{\text{inc}} + u^{\text{scat}}, & x \geq 0. \end{cases} \tag{3.2}$$

Assume that the potential can be written as $V = V_1 + V_2$, where $V_2 = 0$ for $x < 0$, and V_1 is smooth and slowly varying for all x. Let u^{inc} be governed by the TDSE

$$i\varepsilon u_t^{\text{inc}} = -\frac{\varepsilon^2}{2} u_{xx}^{\text{inc}} + V_1 u^{\text{inc}}. \tag{3.3}$$

u^{inc} can then be calculated accurately on the entire domain using Gaussian beams. Given the semidiscretisation

$$i\varepsilon \dot{\mathbf{u}} = -\frac{\varepsilon^2}{2} D\mathbf{u} + V\mathbf{u} \tag{3.4}$$

for the total solution u, where $D = D_2 - P^{-1}S^T B$ is an SBP-SAT discretisation, we get

$$i\varepsilon \dot{\mathbf{v}} = -\frac{\varepsilon^2}{2} D\mathbf{v} + V\mathbf{v} - \frac{\varepsilon^2}{2} \begin{pmatrix} 0 \\ D_R \end{pmatrix} \begin{pmatrix} \mathbf{u}_L^{\text{inc}} \\ \mathbf{0} \end{pmatrix} + \frac{\varepsilon^2}{2} \begin{pmatrix} D_L \\ 0 \end{pmatrix} \begin{pmatrix} \mathbf{0} \\ \mathbf{u}_R^{\text{inc}} \end{pmatrix} \tag{3.5}$$

for v. We have here made the decompositions

$$D = \begin{pmatrix} D_L \\ D_R \end{pmatrix}, \quad \mathbf{u}^{\text{inc}} = \begin{pmatrix} \mathbf{u}_L^{\text{inc}} \\ \mathbf{u}_R^{\text{inc}} \end{pmatrix}, \tag{3.6}$$

where the subscripts L and R denote the restrictions of D and $\mathbf{u}^{\text{inc}}$ to $x < 0$ and $x \geq 0$, respectively. That is, we make row-wise decompositions of D and $\mathbf{u}^{\text{inc}}$. 0 and $\mathbf{0}$ denote zero matrices and zero vectors, respectively, of appropriate size. Eq. (3.5) for $\mathbf{v}$ is then solved, and the total solution $\mathbf{u}$ can be obtained by adding the Gaussian beam solution u^{inc} to $\mathbf{v}$ in $x < 0$. It is straight-forward to derive the error equation, i.e., the time evolution of the pointwise error, and conclude that the Huygens' surface does not introduce any new dominant error source. The leading order error terms will be the truncation error of the SBP operators operating on functions which are smooth, albeit oscillating with wave length of order ε.

3.2 Outflow from the grid

In the outflow buffer, situated directly outside the inflow interface, we construct new Gaussian beams from the grid representation of the scattered part of the solution, u^{scat}. This is done similarly to how the Gaussian beam approximation of the initial condition was constructed, cf. Theorem 2.1, but as a superposition over time instead of over space.

Between the Huygens' surface and the PML we place a buffer region, as wide as the finite difference stencil, which constitutes the outflow buffer. There, at regular time intervals $\Delta\tau$, we spawn outgoing Gaussian beams. We decompose $u^{\text{scat}} = A e^{\mathrm{i}\Phi/\varepsilon}$ in its amplitude and phase, and calculate the first and second order spatial derivatives of the phase Φ using central finite differences. This determines the initial values of the Gaussian beam variables. Denote by Ψ^t the flow of the system (2.3a)-(2.3c), which propagates the Gaussian beam variables, and assume that the Huygens' surface is situated at $x=0$. Then, the Gaussian beam spawned at time $t=\tau$ is given by the function of x and t

$$w(x,t;\tau) = \Psi^{t-\tau} \left(\frac{1}{2\pi\varepsilon}\right)^{1/2} A(0,\tau) \exp\left(\frac{\mathrm{i}}{\varepsilon} T_2^0[\Phi(\cdot,\tau)](x) - \frac{1}{2\varepsilon}x^2\right). \tag{3.7}$$

The Gaussian beam representation of u^{scat} is given by the superposition

$$\int |\Phi_x(0,\tau)| w(x,t;\tau) \mathrm{d}\tau \approx \sum_j \Delta\tau |\Phi_x(0,\tau_j)| w(x,t;\tau_j), \quad \tau_j = j\Delta\tau. \tag{3.8}$$

We scale the amplitude by the momentum $|\Phi_x|$. The reason for this can be understood by comparing to Theorem 2.1, where the superposition was made over the spatial variable x. The momentum is the relation between the spatial and temporal spacing of the beams. In [14], the Gaussian beams were subtracted from the grid representation after being spawned. We leave them on the grid since we would otherwise disturb the spawning of the next Gaussian beam. Instead, we let the outgoing grid solution be consumed by the PML.

Theorem 3.1, which is a time-integral variant of Theorem 2.1, bounds the error from this conversion from point-wise representation to Gaussian beams. It holds when the solution close to the interface consists of a single wave packet propagating out of the finite difference domain. The precise assumptions are as follows. Let $u(x,t)$ be a solution to the free TDSE

$$\mathrm{i}\varepsilon u_t = -\frac{\varepsilon^2}{2} u_{xx} \tag{3.9}$$

with initial condition $u(x,0)$ compactly supported in $x \leq -x_0 < 0$. We write the solution as

$$u(x,t) = A(x,t;\varepsilon) e^{\mathrm{i}\Phi(x,t)/\varepsilon} \tag{3.10}$$

and assume that in a neighbourhood of $\{x=0\}$ the phase Φ, which does not depend on ε, is a solution to the Hamilton–Jacobi equation

$$\Phi_t + \frac{1}{2}\Phi_x^2 = 0. \tag{3.11}$$

For bounding the error at time t, we need Φ to be C^∞ near $\{x=0\}$ during the time interval $[-\delta, t+\delta]$, for some $\delta > 0$ independent of ε. This means that we limit ourselves to the case where no caustics have developed, and the solution is, at least locally around $x=0$, a single wave packet. We further assume that $A(x,t;\varepsilon)$ and $A_t(x,t;\varepsilon)$ can be bounded independently of ε in the same neighbourhood of $\{x=0\}$ and during the same time interval. Finally, we assume that $\Phi_x(0,t) \geq p_0 > 0$, i.e., that we are considering propagation in the positive x-direction, out of the finite difference domain.

Note that global smoothness of Φ would imply the desired bounds for A and A_t. Given (3.9), (3.10) and (3.11), the amplitude $A(x,t;\varepsilon)$ satisfies the equation

$$A_t + \Phi_x A_x + \frac{1}{2}\Phi_{xx}A = \frac{i\varepsilon}{2}A_{xx}, \tag{3.12}$$

which is linear with coefficients in terms of Φ. By standard energy estimate techniques we can then bound A and A_t independently of ε, given that $A(x,0;\varepsilon)$ is smooth and bounded.

Theorem 3.1. *Construct an integral superposition of the time-parametrised Gaussian beams* (3.7),

$$\int_0^{t+\delta} |\Phi_x(0,\tau)| w(x,s;\tau) d\tau, \tag{3.13}$$

over the interval $[0,t+\delta]$, with $\delta \geq \delta_0 > 0$ independent of ε. Then, under the assumptions above, the superposition approximates $u(\cdot,s)$ in $\mathbb{R}^+$ with error bounded by

$$\left\| \int_0^{t+\delta} |\Phi_x(0,\tau)| w(\cdot,s;\tau) d\tau - u(\cdot,s) \right\|_{L_2(\mathbb{R}^+)} \leq C_t \sqrt{\varepsilon}, \tag{3.14}$$

with C_t independent of ε, for all $s \in [0,t]$.

Proof. Given an integral superposition over $[0,t+\delta]$, define the error at time $s \in [0,t]$ as

$$e(x,s) = \int_0^{t+\delta} |\Phi_x(0,\tau)| w(x,s;\tau) d\tau - u(x,s). \tag{3.15}$$

Next we define $g(s) = e(0,s)$, $s \in [0,t]$. The following lemma, which will be proven in the appendix, provides bounds for g and g'.

Lemma 3.1. *Under the assumptions of Theorem 3.1, define*

$$\tilde{u}(s) = \int_0^{t+\delta} |\Phi_x(0,\tau)| w(0,s;\tau) d\tau \tag{3.16}$$

as the integral superposition of Gaussian beams at $x=0$, with $\delta \geq \delta_0 > 0$. Then $\tilde{u}$ approximates u at $x=0$ with error bounded by

$$\|g\|_{L_2([0,t])} = \|\tilde{u}(\cdot) - u(0,\cdot)\|_{L_2([0,t])} \leq C_t \sqrt{\varepsilon}, \tag{3.17}$$

with C_t independent of ε. Furthermore, the time-derivative of the error is bounded by

$$\|g'\|_{L_2([0,t])} = \|\tilde{u}'(\cdot) - u_t(0,\cdot)\|_{L_2([0,t])} \leq C_t \varepsilon^{-1/2}. \tag{3.18}$$

The following lemma, which also will be proven in the appendix, provides a bound on the error growth in terms of g.

Lemma 3.2. *The TDSE quarter-plane problem*

$$i\varepsilon u_t = -\frac{\varepsilon^2}{2}u_{xx}, \qquad\qquad x,t>0, \qquad\qquad (3.19a)$$

$$u(x,0) = f(x), \qquad\qquad f \in L_2, \qquad\qquad (3.19b)$$

$$u(0,t) = g(t), \qquad\qquad g \in H^1, \qquad\qquad (3.19c)$$

where g vanishes at $t=0$, satisfies the energy estimate

$$\|u(\cdot,t)\| \le \|f\| + C(\|g\|_{L_2([0,t])} + \varepsilon\|g'\|_{L_2([0,t])}). \qquad\qquad (3.20)$$

For $x \ge 0$ we have that $e(x,s)$ is a solution to the quarter-plane problem in Lemma 3.2, and is consequently bounded by the energy estimate

$$\|e(\cdot,t)\|_{L_2(\mathbb{R}^+)} \le \|e(\cdot,0)\|_{L_2(\mathbb{R}^+)} + C(\|g\|_{L_2([0,t])} + \varepsilon\|g'\|_{L_2([0,t])})$$

$$\le \|e(\cdot,0)\|_{L_2(\mathbb{R}^+)} + C_t\sqrt{\varepsilon}. \qquad\qquad (3.21)$$

The error at $s=0$ is

$$\|e(\cdot,0)\|_{L_2(\mathbb{R}^+)} = \left\| \int_0^{t+\delta} |\Phi_x(0,\tau)| w(\cdot,0;\tau) d\tau \right\|_{L_2(\mathbb{R}^+)}. \qquad\qquad (3.22)$$

The integral is over the tails of decaying exponentials, and therefore exponentially small in ε. □

4 Time integration

In order to propagate the solution in time we need to integrate the system of ODEs (2.3a)-(2.3c) for each of the Gaussian beams, and the finite difference semidiscretisation of the Schrödinger equation. For the system (2.3a)-(2.3c), which is much cheaper than the finite difference semidiscretisation to integrate, we use the classical fourth order Runge–Kutta method. For the finite difference semidiscretisation we will use an exponential integrator, known as the two-step exponential Gauß rule, which is described below.

The semidiscretisation can be written on the form

$$i\varepsilon\dot{\mathbf{u}} = H\mathbf{u} + \mathbf{F}(t), \qquad\qquad (4.1)$$

where $\mathbf{F}$ is the effect of the Huygens' surface. $\mathbf{F}$ is time-dependent through its dependence on the Gaussian beam solution, cf. (3.5). Given the solution at time t, the solution at time $t+\Delta t$ can be expressed explicitly using the variation-of-constants formula,

$$\mathbf{u}(t+\Delta t) = e^{-i\Delta t H/\varepsilon}\mathbf{u}(t) + \frac{1}{i\varepsilon}\int_0^{\Delta t} e^{-i(\Delta t-\tau)H/\varepsilon}\mathbf{F}(t+\tau)d\tau. \qquad\qquad (4.2)$$

Exponential integrators are constructed by replacing the integral in (4.2) by approximations of it [12]. When working with exponential integrators it is convenient to define the functions

$$\varphi_{k+1}(z) = \frac{\varphi_k(z) - \varphi_k(0)}{z}, \quad \varphi_0(z) = e^z. \tag{4.3}$$

The limit $z \to 0$ exists for all k, and is $1/k!$ for $\varphi_k(z)$.

One class of exponential integrators comprises the exponential quadrature rules,

$$\mathbf{u}_{n+1} = e^{-i\Delta t H/\varepsilon} \mathbf{u}_n + \frac{\Delta t}{i\varepsilon} \sum_{i=1}^{s} b_i\left(\frac{\Delta t}{i\varepsilon} H\right) \mathbf{F}(t_n + c_i \Delta t), \tag{4.4}$$

where the functions $b_i(z)$ are linear combinations of $\varphi_k(z)$. They are suitable for our problem where $\mathbf{F}$ is an inhomogeneity, and not a non-linear term. Since it only depends on the Gaussian beam solution, $\mathbf{F}$ can be computed independently of the finite difference solution. We use the two-step exponential Gauß rule, with $s = 2$, given by

$$b_1(z) = \frac{1+\sqrt{3}}{2}\varphi_1(z) - \sqrt{3}\varphi_2(z), \qquad\qquad c_1 = \frac{1}{2} - \frac{\sqrt{3}}{6}, \tag{4.5a}$$

$$b_2(z) = \frac{1-\sqrt{3}}{2}\varphi_1(z) + \sqrt{3}\varphi_2(z), \qquad\qquad c_2 = \frac{1}{2} + \frac{\sqrt{3}}{6}. \tag{4.5b}$$

This exponential quadrature rule is third order accurate [11, Theorem 2]. In the limit $z \to 0$ it reduces to Gauß-Legendre quadrature. Assuming exact evaluation of all matrix functions, the error bound depends on the norm of $e^{-i\Delta t H/\varepsilon}$ and on the time-derivatives of the inhomogeneous term $\mathbf{F}$, but not on the norm of the Hamiltonian H. Bounds that do not depend on the norm of H are called stiff error estimates. Stiff estimates are desirable since differential operators are unbounded. In particular, the norm of a discretisation of H grows quadratically as the grid spacing is decreased. We compute the action of the matrix functions b_i, as well as the action of the matrix exponential, by Galerkin approximation on the corresponding Krylov subspaces. We generate the Krylov subspaces using the Arnoldi process, and control the error through a residual bound [10].

5 Numerical experiments

5.1 Verification of Theorem 3.1

We here verify the main result Theorem 3.1 with a numerical experiment. We conclude that the result holds, but is pessimistic. In this experiment, we only consider the accuracy of the translation from grid representation to Gaussian beams. The setup is that of Theorem 3.1, with a single outflow interface at $x = 0$. A wave packet approaches from negative x, and is translated to a superposition of Gaussian beams as it crosses the interface.

We use a Gaussian initial condition for the free TDSE (3.9),

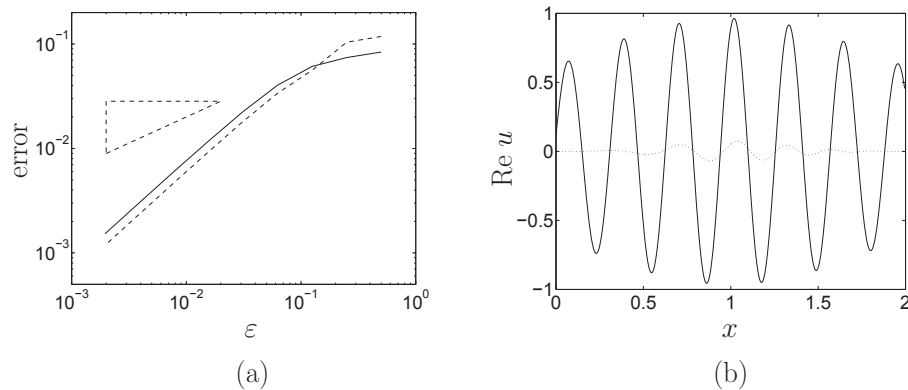$$u(x,0) = \exp\left(-\frac{1}{2}(x+4)^2 + \frac{i}{\varepsilon}(x+4)\right). \tag{5.1}$$

Figure 2: Verification of Theorem 3.1. (a) Error in l_2 (solid) and l_∞ (dashed) norms, as function of ε. The triangle is a reference for order $\varepsilon^{1/2}$ convergence, which is promised by the theorem. The error curves decay linearly in ε. (b) The real part of the solution for $\varepsilon = 0.05$ (solid line). The dotted line shows the contribution of a single Gaussian beam.

We then know the solution for all times, and can compute the amplitude and phase, and its derivatives, analytically. The initial condition does not have compact support as assumed in the theorem, but it is small, $|u(x,0)| \leq \exp(-8)$, for all $x \geq 0$. We use $t=5$ and $\delta=1$, and evaluate the norm of the error at $s=t$, cf. Theorem 3.1. In order to construct the Gaussian beams $w(x,s;\tau)$ we evaluate the analytical solution u at the times $\tau_k = k\Delta\tau$, $\Delta\tau = \varepsilon$, $k = 0, \cdots, (t+\delta)/\Delta\tau$. At each τ_k, a Gaussian beam is spawned at $x=0$ with variables determined from the amplitude-phase decomposition of $u(x,\tau_k) = A\exp(i\Phi/\varepsilon)$. We propagate the spawned beams analytically up to the time $t=5$ and compute the error, the difference between the true solution $u(x,5)$ and the superposition of Gaussian beams, in the interval $0 \leq x < 2$. Note that the beams spawned during $\tau \in (t,t+\delta]$ are propagated backwards in time. The solutions are evaluated and compared on a spatial grid with spacing $\varepsilon/10$, and the error is measured in the l_2 and l_∞ norms. The convergence to the analytical solution of the superposition is shown in Fig. 2. The superposition is well resolved, a reduction of $\Delta\tau$ by a factor 4 would not be noticeable in the figure.

We can conclude that the estimate is pessimistic, we experience first order convergence in ε, to be compared to the promised half-order. This is not unexpected, the same behaviour has been experienced previously for superpositions over the spatial variable. In [24] it was shown how this extra half-order in ε is gained due to error cancellation between adjacent beams in the absence of caustics.

5.2 One-dimensional scattering

In this section we study the scattering of a wave packet by a narrow potential barrier. Such problems are often used as models for chemical reactions. Crossing the barrier corresponds to the reaction happening, and the probability mass that crosses the barrier

gives the reaction probability. We use the Eckart barrier,

$$V(x) = \frac{V_0}{\cosh^2(\alpha x)}, \tag{5.2}$$

with activation energy $V_0 = 0.8$ and the width parameter $\alpha = 40$. The semiclassical parameter $\varepsilon = 10^{-2}$. As initial condition we use a single first order Gaussian beam with

$$a(0) = \sqrt{2}(\pi\varepsilon)^{1/4}, \qquad q(0) = -0.5, \tag{5.3a}$$
$$\phi_0(0) = 0, \qquad p(0) = 1, \tag{5.3b}$$
$$M(0) = i, \tag{5.3c}$$

i.e., a Gaussian wave packet moving towards the barrier. The potential barrier and initial condition are pictured in Fig. 3. This type of problem is difficult to solve with asymptotic methods since the potential has features on a length scale similar to the wave length. The problem also exhibits tunnelling–even though the kinetic energy of the incident wave function is smaller than the activation energy V_0 a significant part of the probability will cross the barrier. Tunnelling is a quantum mechanical phenomenon which is not captured by Gaussian beams.

In the subdomain handled by finite differences we use an SBP operator with internal order of accuracy 6. We place Huygens' surfaces at $x = \pm 0.1$, surrounded by 7 points wide outflow buffers and 20 points wide PMLs. For comparison, the grid between the Huygens' surfaces which is considered necessary for resolving the sharp features of the potential consists of 200 points. For the PMLs we use the parameters $\gamma = \pi/4$, $r = 4$ and $\sigma_0 = 10$, cf. (2.12)-(2.13). Outside the Huygens' surfaces the Gaussian beams propagate according to the full potential V. In the region between the Huygens' surfaces we decompose the potential, $V = V_1 + V_2$, and let V_1 be a second order polynomial which interpolates the Eckart potential V and its derivative at the Huygens' surfaces. The incident beam is propagated according to V_1 between the Huygens' surfaces, while we use the full potential $V_1 + V_2$ for the finite difference method. We do this since the beam, most of which
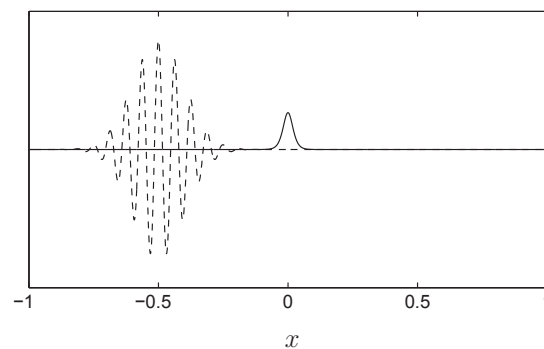
Figure 3: The Eckart potential barrier (solid) and the real part of the initial condition (dashed).
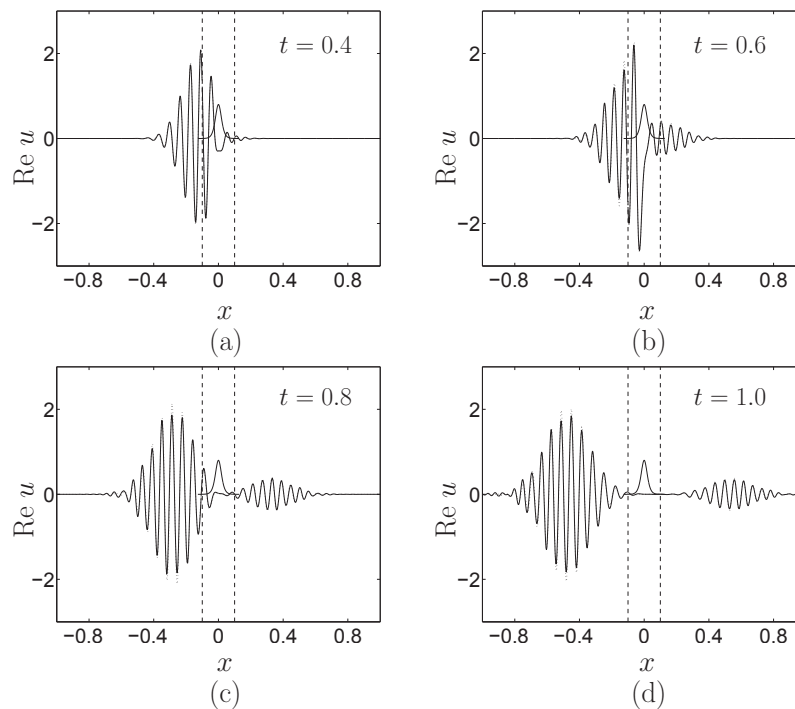
Figure 4: The real parts of the solution of the TDSE with an Eckart potential at different times, using the hybrid method (solid lines) and a reference solution (dotted). The dashed lines show the locations of the Huygens' surfaces, and the potential barrier is illustrated with a solid line. The solutions are very similar, but one can notice that some peaks of the reflected wave function are less sharp for the hybrid method solution.

would already have been translated to grid representation, would otherwise be reflected. Instead, we want the beam to pass through, be translated to grid representation, and let the question of reflection and transmission be handled by the finite difference method. When the tail of the beam at the Huygens' surface is small enough to be neglected we throw the beam away. We keep track of on which side of the barrier the Gaussian beams belong, parts of the incident beam that reaches the far side of the barrier are neglected–they already have a representation on the grid. At the outflow buffers we only spawn new beams if the amplitude is large enough, with the threshold value $|u| \geq 0.01(2\pi\varepsilon)^{1/2}$. In practical computations we typically do not spawn beams at future times to be propagated backwards, i.e., we use $\delta = 0$. This gives an error close to the interface since we lack basis functions on one side of the interface. This error decreases with the beam width, and choosing Im M large reduces this effect further. We use Im $M = 4$.

We solve the problem using the spatial step $\Delta x = \varepsilon/10$ and time step $\Delta t = \varepsilon/100$ for the finite difference method. If the solution amplitude is big enough at the Huygens' surfaces a Gaussian beam is spawned once every 1000 time steps. The solution at times $t = 0.4, 0.6, 0.8$ and 1.0 is shown in Fig. 4. The solution is compared to a reference solution which is computed with the Fourier pseudospectral method in space and Arnoldi time

integration, using the same step lengths as in the finite difference domain. At $t=1$, 16 Gaussian beams have been spawned, and the solution is well represented by the hybrid method. In Fig. 4 we see how a few peaks of the reflected hybrid solution are slightly shorter than in the reference solution, otherwise the two solutions follow each other closely. The domain in which the reference solution is computed is an order of magnitude larger than the finite difference domain of the hybrid method; the hybrid method thereby offers the same reduction in grid size compared to a pure finite difference computation.

5.3   Two-dimensional scattering

We now study a similar example in two dimensions. We embed the Eckart barrier in a harmonic waveguide,

$$V(x,y) = \frac{V_0}{\cosh^2(\alpha x)} + \frac{1}{2}y^2. \tag{5.4}$$

As in the one-dimensional case, $V_0 = 0.8$ and $\alpha = 40$. The potential is depicted in Fig. 5. We use $\varepsilon = 2 \times 10^{-2}$, and as initial condition a single Gaussian beam with

$$a(0) = 2\sqrt{\pi\varepsilon}, \qquad\qquad q(0) = \begin{pmatrix} -0.5 & 0 \end{pmatrix}^T, \tag{5.5a}$$

$$\phi_0(0) = 0, \qquad\qquad p(0) = \begin{pmatrix} 1 & 0 \end{pmatrix}^T, \tag{5.5b}$$

$$M(0) = iI. \tag{5.5c}$$

We use SBP operators with internal order of accuracy 6, and in the x-direction we construct the interfaces as in the one-dimensional case. The waveguide confines the wave function in a strip along the x-axis, we can therefore use homogeneous Dirichlet boundary conditions in the y-direction.
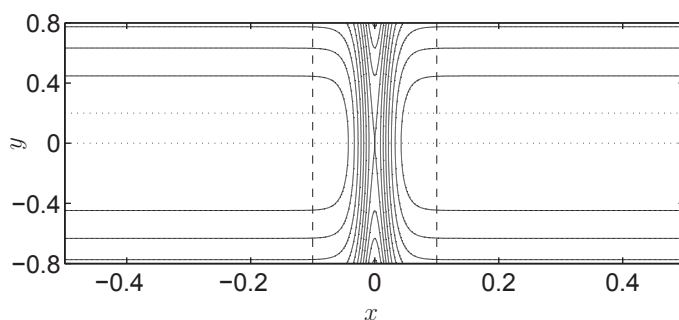

Figure 5: Level curves for the potential (5.4), with separation 0.1. The dashed lines indicates the position of the Huygens' surfaces, and the dotted lines the cross sections plotted in Fig. 6.

For the outflow interface, the superposition is an integral over space along the interface and over time normal to it, i.e., at each of the two interfaces, the Gaussian beam superposition is created from the pointwise solution as

$$\tilde{u}(x,y,t) = \iint |\nabla\Phi(0,y,\tau) \cdot \hat{x}| w(x,y,t;\tau) d\tau dy. \tag{5.6}$$
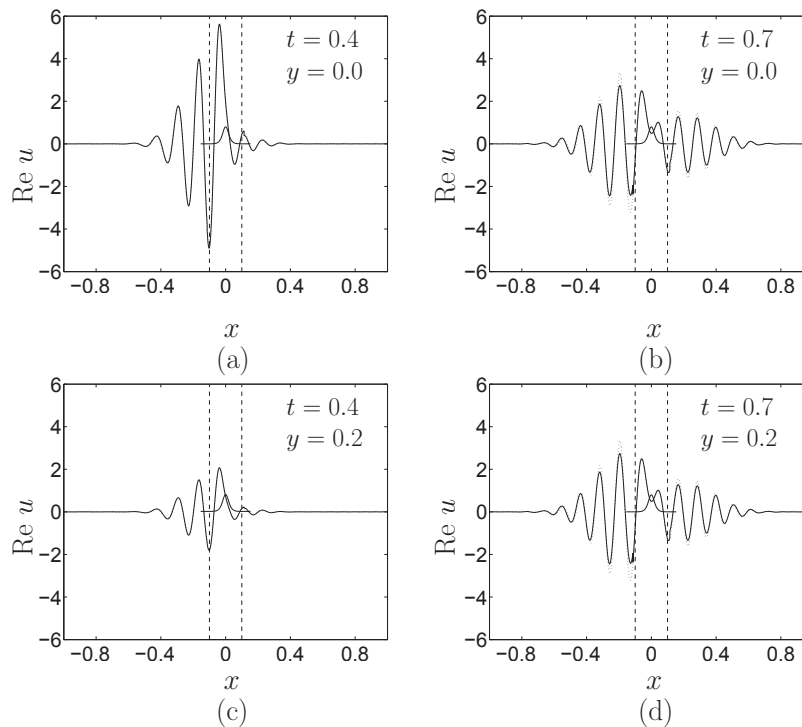
Figure 6: The real parts of the solution of the two-dimensional TDSE with an Eckart barrier in a harmonic waveguide, using the new method (solid lines) and a reference solution (dotted). The cross section $y = 0.0$ of the solution is shown at times (a) $t = 0.4$, (b) $t = 0.7$, and the cross section $y = 0.2$ is shown at the same times in (c) and (d). The dashed lines show the locations of the Huygens' surfaces, and the potential barrier is illustrated with a solid line segment.

$\hat{x}$ denotes the unit vector normal to the interface.

We solve the problem using the spatial steps $\Delta x = \varepsilon/10$, $\Delta y = \varepsilon$, and the time step $\Delta t = \varepsilon/100$ for the finite difference method. The Huygens' surfaces are located at $x = \pm 0.1$, and the grid is truncated in the y-coordinate at $y = \pm 0.8$. If the solution amplitude is big enough at the Huygens' surfaces a Gaussian beam is spawned once every 500 time steps, and at every four grid points in the y-direction along the interfaces. We used the spawning threshold $|u| \geq 0.01(2\pi\varepsilon)^{1/2}$, and Im $M = 4$, as in the one-dimensional case. Cross sections of the solution at times $t = 0.4$ and $t = 0.7$ are shown in Fig. 6. The solution is compared to a reference solution which is computed with the Fourier pseudospectral method in space and Arnoldi time integration, using the same step lengths as in the finite difference domain.

6   Conclusions

Numerical solution of the time-dependent Schrödinger equation in the semiclassical

regime is notoriously expensive due to oscillations in the solution with very short wave length. Approximate, asymptotic methods such as Gaussian beams provide an efficient alternative to direct methods like finite differences or pseudospectral methods. They do however not perform well in regions where the potential has variations on a short length scale.

We have constructed a hybrid method which uses Gaussian beams in most of the domain, and a finite difference method in regions where the potential has strong variations. The method is similar to the one presented in [14], but handles the coupling between the two methods in a different way. For the price of stronger assumptions on the potential we reduce the cost of the coupling considerably. To translate Gaussian beams to a grid representation we use Huygens' surfaces, and for coupling in the other direction we use a result for the construction of integral superpositions of Gaussian beams. This reduces the size of the buffer regions needed in the interfaces substantially, and thereby reduces the size of the part of the domain where the more expensive finite difference method has to be used. Potential applications include photodissociation and reactive scattering problems. The extension to curvilinear grids, for two-dimensional problems with more complicated geometry than the one studied in Section 5.3, is straight-forward. However, the parts of the boundary where the solution transits between the two representations need to be smooth. For a problem with several reaction channels, this can be handled by placing the corners of the grid up on a potential hillside, in a dead angle where little happens.

Appendix: proofs of the lemmas

We here prove the lemmas used in the proof of Theorem 3.1. We start with Lemma 3.1, which bounds the error of the Gaussian beam superposition at the outflow interface. Thereafter we prove Lemma 3.2, which is an energy estimate for the TDSE initial-boundary-value problem.

A.1   Proof of Lemma 3.1

Define shorthand notation for the variables of a Gaussian beam spawned at $x = 0$, $t = \tau$ as

$$a_\tau = A(0,\tau), \qquad\qquad H_\tau = \Phi_{xx}(0,\tau), \qquad\qquad \text{(A.1a)}$$

$$\phi_{0,\tau} = \Phi(0,\tau), \qquad\qquad M_\tau = H_\tau + i, \qquad\qquad \text{(A.1b)}$$

$$p_\tau = \Phi_x(0,\tau). \qquad\qquad\qquad\qquad \text{(A.1c)}$$

We start with proving the bound (3.17). We use the analytical solution of the system of ODEs (2.3a)-(2.3c) with $V \equiv 0$,

$$a(t) = \frac{a_\tau}{\sqrt{1 + M_\tau(t-\tau)}}, \qquad\qquad q(t) = q_\tau + p_\tau(t-\tau), \qquad\qquad \text{(A.2a)}$$

$$\phi_0(t) = \phi_{0,\tau} + \frac{1}{2}p_\tau^2(t-\tau), \qquad\qquad p(t) = p_\tau, \qquad\qquad \text{(A.2b)}$$

$$M(t) = \frac{M_\tau}{1+M_\tau(t-\tau)}. \qquad\qquad \text{(A.2c)}$$

We then get

$$
\begin{aligned}
\tilde{u}(s) &= \int_0^{t+\delta} |p_\tau| w(0,s;\tau)\mathrm{d}\tau \\
&= \int_0^{t+\delta} |p_\tau| \left(\frac{1}{2\pi\varepsilon}\right)^{1/2} \frac{a_\tau}{\sqrt{1+M_\tau(s-\tau)}} \times \exp\left(\frac{\mathrm{i}}{\varepsilon}\left(\phi_{0,\tau} + \frac{1}{2}p_\tau^2(s-\tau) + p_\tau(-p_\tau(s-\tau))\right.\right. \\
&\qquad\left.\left. + \frac{1}{2}\frac{M_\tau}{1+M_\tau(s-\tau)}(-p_\tau(s-\tau))^2\right)\right)\mathrm{d}\tau \\
&= \int_0^{t+\delta} |p_\tau| \left(\frac{1}{2\pi\varepsilon}\right)^{1/2} \frac{a_\tau}{\sqrt{1+M_\tau(s-\tau)}} \\
&\qquad \times \exp\left(\frac{\mathrm{i}}{\varepsilon}\left(\phi_{0,\tau} - \frac{1}{2}p_\tau^2(s-\tau) + \frac{1}{2}\frac{M_\tau}{1+M_\tau(s-\tau)}p_\tau^2(s-\tau)^2\right)\right)\mathrm{d}\tau. \qquad \text{(A.3)}
\end{aligned}
$$

Let $\alpha(\tau,s-\tau) = p_\tau^2(1+M_\tau(s-\tau))^{-1}$. Then,

$$
\begin{aligned}
\tilde{u}(s) &= \int_0^{t+\delta} \left(\frac{\alpha(\tau,s)}{2\pi\varepsilon}\right)^{1/2} a_\tau \exp\left(\frac{\mathrm{i}}{\varepsilon}\left(\phi_{0,\tau} - \frac{1}{2}p_\tau^2(s-\tau)\right.\right. \\
&\qquad\left.\left. + \frac{1}{2}\frac{p_\tau^2 H_\tau}{1+M_\tau(s-\tau)}(s-\tau)^2\right) - \frac{\alpha(\tau,s)}{2\varepsilon}(s-\tau)^2\right)\mathrm{d}\tau \\
&= \int_0^{t+\delta} \left(\frac{\alpha(\tau,s)}{2\pi\varepsilon}\right)^{1/2} a_\tau \exp\left(\frac{\mathrm{i}}{\varepsilon}\left(\phi_{0,\tau} - \frac{1}{2}p_\tau^2(s-\tau) + \frac{1}{2}p_\tau^2 H_\tau(s-\tau)^2\right.\right. \\
&\qquad\left.\left. - \frac{1}{2}\frac{p_\tau^2 H_\tau M_\tau(s-\tau)}{1+M_\tau(s-\tau)}(s-\tau)^2\right) - \frac{\alpha(\tau,s)}{2\varepsilon}(s-\tau)^2\right)\mathrm{d}\tau \\
&= \int_0^{t+\delta} \left(\frac{\alpha(\tau,s)}{2\pi\varepsilon}\right)^{1/2} A(0,\tau) \exp\left(\frac{\mathrm{i}}{\varepsilon}\left(\Phi(0,\tau) - \frac{1}{2}\Phi_x^2(0,\tau)(s-\tau)\right.\right. \\
&\qquad\left.\left. + \frac{1}{2}\Phi_x^2\Phi_{xx}(s-\tau)^2\right) - \frac{\beta(\tau,s)}{2\varepsilon}(s-\tau)^2\right)\mathrm{d}\tau, \qquad \text{(A.4)}
\end{aligned}
$$

where we have defined

$$\beta(\tau,s) = \alpha(\tau,s) + \mathrm{i}\frac{p_\tau^2 H_\tau M_\tau(s-\tau)}{1+M_\tau(s-\tau)}. \qquad\qquad \text{(A.5)}$$

The phase $\Phi(x,t)$ of the exact solution $u(x,t)$ satisfies the Hamilton-Jacobi equation (3.11) in a neighbourhood of $\{x=0\}$. Differentiation of (3.11) with respect to time gives

$$\Phi_{tt} = \Phi_x^2\Phi_{xx}. \qquad\qquad \text{(A.6)}$$

We use this to exchange the spatial derivatives of Φ for temporal ones,

$$
\begin{aligned}
\tilde{u}(s) =& \int_0^{t+\delta} \left(\frac{\alpha(\tau,s)}{2\pi\varepsilon}\right)^{1/2} A(0,\tau) \exp\left(\frac{\mathrm{i}}{\varepsilon}\left(\Phi(0,\tau)+\Phi_t(0,\tau)(s-\tau)\right.\right.\\
&\left.\left.+\frac{1}{2}\Phi_{tt}(0,\tau)(s-\tau)^2\right)-\frac{\beta(\tau,s)}{2\varepsilon}(s-\tau)^2\right)\mathrm{d}\tau \\
=& \int_0^{t+\delta} \left(\frac{\alpha(\tau,s)}{2\pi\varepsilon}\right)^{1/2} A(0,\tau) \times \exp\left(\frac{\mathrm{i}}{\varepsilon}T_2^\tau[\Phi(0,\cdot)](s)-\frac{\beta(\tau,s)}{2\varepsilon}(s-\tau)^2\right)\mathrm{d}\tau. \quad\text{(A.7)}
\end{aligned}
$$

In order to prove the estimate we need a bound $\operatorname{Re}\beta(\tau,s)\geq\beta_0>0$, so that the integrand has a Gaussian shape. We can indeed prove such a bound,

$$
\begin{aligned}
\operatorname{Re}\beta =& \operatorname{Re}\left(\frac{p_\tau^2}{1+M_\tau(s-\tau)}+\mathrm{i}\frac{p_\tau^2 H_\tau M_\tau(s-\tau)}{1+M_\tau(s-\tau)}\right) \\
=& p_\tau^2 \operatorname{Re}\frac{(1+\mathrm{i}H_\tau M_\tau(s-\tau))(1+M_\tau^*(s-\tau))}{|1+M_\tau(s-\tau)|^2} \\
=& \frac{p_\tau^2}{|1+M_\tau(s-\tau)|^2}\operatorname{Re}\left(1+M_\tau^*(s-\tau)+\mathrm{i}H_\tau M_\tau(s-\tau)+\mathrm{i}H_\tau|M_\tau|^2(s-\tau)^2\right) \\
=& \frac{p_\tau^2}{|1+M_\tau(s-\tau)|^2}\operatorname{Re}\left(1+(H_\tau-\mathrm{i})(s-\tau)+\mathrm{i}H_\tau(H_\tau+\mathrm{i})(s-\tau)\right) \\
=& \frac{p_\tau^2}{|1+M_\tau(s-\tau)|^2}, \quad\text{(A.8)}
\end{aligned}
$$

which is strictly positive for finite s and τ.

The remainder of proof resembles the proof for [31, Theorem 2.1]. We elaborate on the deviation of $\tilde{u}$ from the exact solution,

$$
\begin{aligned}
e(0,s) =& \tilde{u}(s)-u(0,s) \\
=& \int_0^{t+\delta}\left(\frac{\alpha(\tau,s)}{2\pi\varepsilon}\right)^{1/2}A(0,\tau)\exp\left(\frac{\mathrm{i}}{\varepsilon}T_2^\tau[\Phi(0,\cdot)](s)\right.\\
&\left.-\frac{\beta(\tau,s)}{2\varepsilon}(s-\tau)^2\right)\mathrm{d}\tau - A(0,s)\exp\left(\frac{\mathrm{i}}{\varepsilon}\Phi(0,s)\right), \quad\text{(A.9a)}\\
|e(0,s)| =& \left|\int_0^{t+\delta}\left(\frac{\alpha(\tau,s)}{2\pi\varepsilon}\right)^{1/2}A(0,\tau)\right.\\
&\left.\times\exp\left(-\frac{\mathrm{i}}{\varepsilon}R_2^\tau[\Phi(0,\cdot)](s)-\frac{\beta(\tau,s)}{2\varepsilon}(s-\tau)^2\right)\mathrm{d}\tau - A(0,s)\right|. \quad\text{(A.9b)}
\end{aligned}
$$

We need to extend the interval of the above integral to $\tau\in[-\delta,t+\delta]$, otherwise the result will not hold for times s close to 0. Due to the compact support of the initial condition, $A(0,0)=0$. By Taylor expanding A around $\tau=0$ one can show that

$$
\left|\int_{-\delta}^0\left(\frac{\alpha(\tau,s)}{2\pi\varepsilon}\right)^{1/2}A(0,\tau)\exp\left(-\frac{\mathrm{i}}{\varepsilon}R_2^\tau[\Phi(0,\cdot)](s)-\frac{\beta(\tau,s)}{2\varepsilon}(s-\tau)^2\right)\mathrm{d}\tau\right|
$$

$$\leq C\varepsilon^{-1/2}\int_{-\delta}^{0}|\tau|e^{-\beta_0\tau^2/(2\varepsilon)}d\tau\leq C\sqrt{\varepsilon}. \tag{A.10}$$

In the last step we used the estimate

$$\int_{-\infty}^{\infty}|x|^p e^{-cx^2/\varepsilon}dx\leq C\varepsilon^{(p+1)/2}, \quad c>0, \quad p\geq 0. \tag{A.11}$$

The constant C does not depend on ε, and since the integrand is non-negative the bound holds also for finite intervals. We will frequently use this bound, with $c=\beta_0/2$. We can then make the extension of the interval, and get

$$|e(0,s)|=\left|\int_{-\delta}^{t+\delta}\left(\frac{\alpha(\tau,s)}{2\pi\varepsilon}\right)^{1/2}A(0,\tau)\exp\left(-\frac{i}{\varepsilon}R_2^\tau[\Phi(0,\cdot)](s)\right.\right.$$
$$\left.\left.-\frac{\beta(\tau,s)}{2\varepsilon}(s-\tau)^2\right)d\tau-A(0,s)\right|+C\sqrt{\varepsilon}. \tag{A.12}$$

We will also need a bound on the following expression, which will follow from Taylor expansion of $\alpha(\tau,s)$ and $\beta(\tau,s)$ around $\tau=s$,

$$\left|\int_{-\delta}^{t+\delta}\left(\frac{\alpha(\tau,s)}{2\pi\varepsilon}\right)^{1/2}\exp\left(-\frac{\beta(\tau,s)}{2\varepsilon}(s-\tau)^2\right)d\tau-1\right|$$
$$\leq\left|\int_{-\delta}^{t+\delta}\left(\frac{\alpha(s,s)}{2\pi\varepsilon}\right)^{1/2}\exp\left(-\frac{\beta(s,s)}{2\varepsilon}(s-\tau)^2\right)d\tau-1\right|$$
$$+\int_{-\delta}^{t+\delta}\frac{|\alpha(\tau,s)^{1/2}-\alpha(s,s)^{1/2}|}{(2\pi\varepsilon)^{1/2}}\exp\left(-\frac{\beta(s,s)}{2\varepsilon}(s-\tau)^2\right)d\tau$$
$$+\int_{-\delta}^{t+\delta}\left(\frac{\alpha(\tau,s)}{2\pi\varepsilon}\right)^{1/2}\left|e^{-\frac{\beta(\tau,s)}{2\varepsilon}(s-\tau)^2}-e^{-\frac{\beta(s,s)}{2\varepsilon}(s-\tau)^2}\right|d\tau$$
$$\equiv I_1+I_2+I_3. \tag{A.13}$$

We estimate the integrals separately, starting with I_1. Since $\alpha(s,s)=\beta(s,s)$ and $s\in[0,t]$, a change of variables $\tau\mapsto s+\tau\sqrt{2\varepsilon/\alpha(s,s)}$ gives

$$I_1=\left|\frac{1}{\sqrt{\pi}}\int_{\frac{-\delta-s}{\sqrt{2\varepsilon/\alpha(s,s)}}}^{\frac{\delta+t-s}{\sqrt{2\varepsilon/\alpha(s,s)}}}e^{-\tau^2}d\tau-1\right|\leq\frac{1}{\sqrt{\pi}}\int_{|\tau|\geq\frac{\delta}{\sqrt{2\varepsilon/\alpha(s,s)}}}e^{-\tau^2}d\tau$$
$$\leq\frac{1}{\sqrt{\pi}}\int_{-\infty}^{\infty}e^{-\tau^2-\frac{\delta^2\alpha(s,s)}{2\varepsilon}}d\tau=e^{-\frac{\delta^2\alpha(s,s)}{2\varepsilon}}\leq C_r\varepsilon^r, \tag{A.14}$$

for any $r>0$. For I_2 we can bound $|\alpha(\tau,s)^{1/2}-\alpha(s,s)^{1/2}|\leq C|\tau-s|$ in the integration interval, to get

$$I_2\leq\frac{C}{\sqrt{\varepsilon}}\int_{-\delta}^{t+\delta}|s-\tau|\exp\left(-\frac{\beta_0}{2\varepsilon}(s-\tau)^2\right)d\tau\leq C\sqrt{\varepsilon}, \tag{A.15}$$

by also using (A.11). Finally, for I_3 we have by the mean value theorem applied to $z \mapsto \exp(-\beta(z,s)(s-\tau)^2/2\varepsilon)$,

$$
e^{-\frac{\beta(\tau,s)}{2\varepsilon}(s-\tau)^2} - e^{-\frac{\beta(s,s)}{2\varepsilon}(s-\tau)^2} = \frac{\beta_\tau(\xi,s)}{2\varepsilon}(s-\tau)^3 e^{-\frac{\beta(\xi,s)}{2\varepsilon}(s-\tau)^2} \tag{A.16}
$$

for some ξ between τ and s. Hence, by (A.11) again

$$
I_3 \leq \frac{C}{\varepsilon^{3/2}} \int_{-\delta}^{t+\delta} |s-\tau|^3 e^{-\frac{\beta_0}{2\varepsilon}(s-\tau)^2} \mathrm{d}\tau \leq C\sqrt{\varepsilon}. \tag{A.17}
$$

In conclusion,

$$
\left| \int_{-\delta}^{t+\delta} \left(\frac{\alpha(\tau,s)}{2\pi\varepsilon} \right)^{1/2} \exp\left(-\frac{\beta(\tau,s)}{2\varepsilon}(s-\tau)^2 \right) \mathrm{d}\tau - 1 \right| \leq C\sqrt{\varepsilon}. \tag{A.18}
$$

Now, using (A.18),

$$
\begin{aligned}
|e(0,s)| \leq \Bigg| & \int_{-\delta}^{t+\delta} \left(\frac{\alpha(\tau,s)}{2\pi\varepsilon} \right)^{1/2} A(0,\tau) \exp\left(-\frac{\mathrm{i}}{\varepsilon} R_2^\tau[\Phi(0,\cdot)](s) - \frac{\beta(\tau,s)}{2\varepsilon}(s-\tau)^2 \right) \mathrm{d}\tau \\
& - A(0,s) \int_{-\delta}^{t+\delta} \left(\frac{\alpha(\tau,s)}{2\pi\varepsilon} \right)^{1/2} \exp\left(-\frac{\beta(\tau,s)}{2\varepsilon}(s-\tau)^2 \right) \mathrm{d}\tau \Bigg| + C\sqrt{\varepsilon} \\
\leq \Bigg| & \int_{-\delta}^{t+\delta} \left(\frac{\alpha(\tau,s)}{2\pi\varepsilon} \right)^{1/2} (A(0,\tau) - A(0,s) \exp\left(-\frac{\mathrm{i}}{\varepsilon} R_2^\tau[\Phi(0,\cdot)](s) - \frac{\beta(\tau,s)}{2\varepsilon}(s-\tau)^2 \right) \mathrm{d}\tau \Bigg| \\
& + \Bigg| A(0,s) \int_{-\delta}^{t+\delta} \left(\frac{\alpha(\tau,s)}{2\pi\varepsilon} \right)^{1/2} \exp\left(-\frac{\beta(\tau,s)}{2\varepsilon}(s-\tau)^2 \right) \\
& \times \left(\exp\left(-\frac{\mathrm{i}}{\varepsilon} R_2^\tau[\Phi(0,\cdot)](s) \right) - 1 \right) \mathrm{d}\tau \Bigg| + C\sqrt{\varepsilon}. \tag{A.19}
\end{aligned}
$$

The expression (A.19) consists of three terms, which we denote as $|e(0,s)| \leq I_4 + I_5 + C\sqrt{\varepsilon}$ and bound one by one. Since $\alpha(s,s) = \beta(s,s)$ and $\mathrm{Re}\,\beta(\tau,s) \geq \beta_0 > 0$, the integrands have Gaussian shape. This makes it possible to control the remainder terms of the Taylor expansions using (A.11). Starting with I_4, which we bound by Taylor expanding $A(0,\tau)$ around $\tau = s$,

$$
I_4 \leq C\varepsilon^{-1/2} \int_{-\delta}^{t+\delta} |\tau-s| \exp\left(-\frac{\beta_0}{2\varepsilon}(s-\tau)^2 \right) \mathrm{d}\tau \leq C\sqrt{\varepsilon}. \tag{A.20}
$$

Using the inequality $|\exp(\mathrm{i}x) - 1| \leq |x|$, $x \in \mathbb{R}$, we can bound I_5 as

$$
\begin{aligned}
I_5 & \leq C\varepsilon^{-1/2} \int_{-\delta}^{t+\delta} \exp\left(-\frac{\beta_0}{2\varepsilon}(s-\tau)^2 \right) \left| \varepsilon^{-1} R_2^\tau[\Phi(0,\cdot)](s) \right| \mathrm{d}\tau \\
& \leq C\varepsilon^{-3/2} \int_{-\delta}^{t+\delta} |s-\tau|^3 \exp\left(-\frac{\beta_0}{2\varepsilon}(s-\tau)^2 \right) \mathrm{d}\tau \\
& \leq C\sqrt{\varepsilon}. \tag{A.21}
\end{aligned}
$$

Adding the contributions yields

$$|e(0,s)| \leq C\sqrt{\varepsilon}. \tag{A.22}$$

We thus have a bound for the maximum norm of the error. We then also have an L_2 bound of the same type since the interval is finite, and we have thereby proven (3.17).

For bounding the derivative of the error as in (3.18) we differentiate $\tilde{u}(s)$ as expressed in (A.7). The derivatives of α and β with respect to s are

$$\frac{\partial \alpha}{\partial s} = -\frac{p_\tau^2 M_\tau}{(1+M_\tau(s-\tau))^2}, \quad \frac{\partial \beta}{\partial s} = \frac{ip_\tau^2 H_\tau M_\tau - p_\tau^2 M_\tau}{(1+M_\tau(s-\tau))^2}. \tag{A.23}$$

We then get

$$\begin{aligned}
\tilde{u}'(s) &= \int_0^{t+\delta} \left(\frac{\alpha(\tau,s)}{2\pi\varepsilon}\right)^{1/2} A(0,\tau) \left(\frac{\pi\varepsilon}{\alpha(\tau,s)}\frac{\partial \alpha}{\partial s} + \frac{i}{\varepsilon}T_1^\tau[\Phi_t(0,\cdot)](s) - \frac{\partial\beta/\partial s}{2\varepsilon}(s-\tau)^2 \right. \\
&\quad \left. -\frac{\beta(\tau,s)}{\varepsilon}(s-\tau)\right) \times \exp\left(\frac{i}{\varepsilon}T_2^\tau[\Phi(0,\cdot)](s) - \frac{\beta(\tau,s)}{2\varepsilon}(s-\tau)^2\right) d\tau \\
&= \int_0^{t+\delta} \left(\frac{\alpha(\tau,s)}{2\pi\varepsilon}\right)^{1/2} A(0,\tau) \times \left(-\frac{\pi\varepsilon M_\tau}{1+M_\tau(s-\tau)} + \frac{i}{\varepsilon}T_1^\tau[\Phi_t(0,\cdot)](s)\right. \\
&\quad \left. -\frac{1}{2\varepsilon}\frac{ip_\tau^2 H_\tau M_\tau - p_\tau^2 M_\tau}{(1+M_\tau(s-\tau))^2}(s-\tau)^2 - \frac{1}{\varepsilon}\frac{p_\tau^2 + ip_\tau^2 H_\tau M_\tau(s-\tau)}{1+M_\tau(s-\tau)}(s-\tau)\right) \\
&\quad \times \exp\left(\frac{i}{\varepsilon}T_2^\tau[\Phi(0,\cdot)](s) - \frac{\beta(\tau,s)}{2\varepsilon}(s-\tau)^2\right) d\tau. \tag{A.24}
\end{aligned}$$

We next use (A.11) to get rid of the small terms,

$$\begin{aligned}
\tilde{u}'(s) &= \frac{i}{\varepsilon}\int_{-\delta}^{t+\delta} \left(\frac{\alpha(\tau,s)}{2\pi\varepsilon}\right)^{1/2} A(0,\tau)T_1^\tau[\Phi_t(0,\cdot)](s) \\
&\quad \times \exp\left(\frac{i}{\varepsilon}T_2^\tau[\Phi(0,\cdot)](s) - \frac{\beta(\tau,s)}{2\varepsilon}(s-\tau)^2\right) d\tau + \mathcal{O}(\varepsilon^{-1/2}). \tag{A.25}
\end{aligned}$$

We also extended the integration interval to $\tau \in [-\delta, t+\delta]$ above. This can be justified by Taylor expanding $A(0,\tau)$ as in (A.10), it induces an error of order $\varepsilon^{-1/2}$. Using the same techniques as when bounding $e(0,s)$, the deviation of $\tilde{u}'$ from $u_t(0,\cdot)$ is bounded by

$$\begin{aligned}
|e_s(0,s)| &= |\tilde{u}'(s) - u_t(0,s)| \\
&\leq \left|\frac{i}{\varepsilon}\int_{-\delta}^{t+\delta} \left(\frac{\alpha(\tau,s)}{2\pi\varepsilon}\right)^{1/2} A(0,\tau)T_1^\tau[\Phi_t(0,\cdot)](s) \times \exp\left(\frac{i}{\varepsilon}T_2^\tau[\Phi(0,\cdot)](s)\right. \right. \\
&\quad \left. \left. -\frac{\beta(\tau,s)}{2\varepsilon}(s-\tau)^2\right) d\tau - \left(A_t(0,s) + \frac{i}{\varepsilon}A(0,s)\Phi_t(0,s)\right)\exp\left(\frac{i}{\varepsilon}\Phi(0,s)\right)\right| + C\varepsilon^{-1/2} \\
&\leq \left|\frac{i}{\varepsilon}\int_{-\delta}^{t+\delta} \left(\frac{\alpha(\tau,s)}{2\pi\varepsilon}\right)^{1/2} A(0,\tau)T_1^\tau[\Phi_t(0,\cdot)](s) \right. \\
&\quad \left. \times \exp\left(-\frac{i}{\varepsilon}R_2^\tau[\Phi(0,\cdot)](s) - \frac{\beta(\tau,s)}{2\varepsilon}(s-\tau)^2\right) d\tau - \frac{i}{\varepsilon}A(0,s)\Phi_t(0,s)\right| + C\varepsilon^{-1/2}
\end{aligned}$$

$$\leq \left| \frac{i}{\varepsilon} \int_{-\delta}^{t+\delta} \left(\frac{\alpha(s,s)}{2\pi\varepsilon} \right)^{1/2} A(0,\tau) T_1^\tau [\Phi_t(0,\cdot)](s) \times \exp\left(-\frac{\alpha(s,s)}{2\varepsilon}(s-\tau)^2 \right) d\tau \right.$$

$$\left. -\frac{i}{\varepsilon} A(0,s)\Phi_t(0,s) \right| + C\varepsilon^{-1/2}$$

$$\leq C\varepsilon^{-1/2}. \tag{A.26}$$

Thus, we complete the proof.   □

A.2   Proof of Lemma 3.2

We start by considering the problem with homogeneous initial condition. We then want to bound the solution to the quarter-plane problem

$$u_t = \frac{i\varepsilon}{2} u_{xx}, \qquad\qquad x,t>0, \tag{A.27a}$$

$$u(0,t) = g(t), \qquad\qquad g \in H^1([0,\infty)), \tag{A.27b}$$

$$u(x,0) = 0, \tag{A.27c}$$

in terms of ε and the boundary condition g. g is assumed to vanish at $t=0$. Define the Laplace transform,

$$\hat{f}(s) = \int_0^\infty e^{-st} f(t) dt, \quad f \in L_2. \tag{A.28}$$

Laplace transforming the problem (A.27a)-(A.27c) in time yields

$$s\hat{u} = \frac{i\varepsilon}{2} \hat{u}_{xx}, \quad \hat{u}(0,s) = \hat{g}(s), \tag{A.29}$$

an ODE in x which we can solve. The solution is

$$\hat{u}(x,s) = \hat{g}(s)e^{\kappa(s)x}, \quad \kappa = \sqrt{-\frac{2is}{\varepsilon}}, \tag{A.30}$$

where the branch of the square root is taken such that κ is in the second quadrant of the complex plane for all $s = \eta + i\xi$ with $\eta > 0$. The solution to the original problem (A.27a)-(A.27c) is given by the inverse Laplace transform, for fixed $\eta > 0$,

$$u(x,t) = \frac{1}{2\pi} \int_{-\infty}^\infty e^{st} \hat{u}(x,s) d\xi = \frac{1}{2\pi} \int_{-\infty}^\infty e^{st} e^{\kappa x} \hat{g}(s) d\xi. \tag{A.31}$$

We evaluate this expression in the limit $\eta \to 0$, where

$$\kappa(i\xi) = \begin{cases} i\sqrt{-2\xi/\varepsilon}, & \xi < 0, \\ -\sqrt{2\xi/\varepsilon}, & \xi > 0. \end{cases} \tag{A.32}$$

This invites us to split the interval of the integral (A.31) in positive and negative ξ,

$$u(x,t) = \frac{1}{2\pi} \int_{-\infty}^{0} e^{i\xi t} e^{i\sqrt{-2\xi/\varepsilon}x} \hat{g}(i\xi) d\xi + \frac{1}{2\pi} \int_{0}^{\infty} e^{i\xi t} e^{-\sqrt{2\xi/\varepsilon}x} \hat{g}(i\xi) d\xi. \tag{A.33}$$

We denote the two terms in the right-hand side of (A.33) by u_- and u_+ and bound them separately, starting with

$$u_-(x,t) = \frac{1}{2\pi} \int_{-\infty}^{0} e^{i\xi t} e^{i\sqrt{-2\xi/\varepsilon}x} \hat{g}(i\xi) d\xi, \tag{A.34a}$$

$$\|u_-(\cdot,t)\|^2 = \int_{0}^{\infty} \left| \frac{1}{2\pi} \int_{-\infty}^{0} e^{i\xi t} e^{i\sqrt{-2\xi/\varepsilon}x} \hat{g}(i\xi) d\xi \right|^2 dx. \tag{A.34b}$$

Let $\sigma(\xi) = \sqrt{-2\xi/\varepsilon}$, $\xi = \phi(\sigma) = -\varepsilon\sigma^2/2$, and substitute variables,

$$\|u_-(\cdot,t)\|^2 = \frac{1}{4\pi^2} \int_{0}^{\infty} \left| \int_{0}^{\infty} e^{i\sigma x} e^{i\phi(\sigma)t} \hat{g}(i\phi(\sigma)) \phi'(\sigma) d\sigma \right|^2 dx. \tag{A.35}$$

Define $F(\sigma) = e^{i\phi(\sigma)t} \hat{g}(i\phi(\sigma)) \phi'(\sigma)$ for $\sigma \geq 0$, and extend its domain to the whole real axis by letting $F(\sigma) = 0$ for all $\sigma < 0$. We then recognise a Fourier transform, and may apply Parseval's relation.

$$\begin{aligned}
\|u_-(\cdot,t)\|^2 &= \frac{1}{4\pi^2} \int_{0}^{\infty} \left| \int_{0}^{\infty} e^{i\sigma x} F(\sigma) d\sigma \right|^2 dx \leq \frac{1}{4\pi^2} \int_{-\infty}^{\infty} \left| \int_{-\infty}^{\infty} e^{i\sigma x} F(\sigma) d\sigma \right|^2 dx \\
&= \frac{1}{2\pi} \int_{-\infty}^{\infty} |F(\sigma)|^2 d\sigma = \frac{1}{2\pi} \int_{0}^{\infty} |\hat{g}(i\phi(\sigma))|^2 (\phi'(\sigma))^2 d\sigma \\
&= \frac{1}{2\pi} \int_{-\infty}^{0} |\hat{g}(i\xi)|^2 \sqrt{-2\varepsilon\xi} d\xi \leq C\sqrt{\varepsilon} \int_{-\infty}^{\infty} |\xi^{1/4} \hat{g}(i\xi)|^2 d\xi. \tag{A.36}
\end{aligned}$$

If we apply the Parseval relation to the last integral, we get an expression including the 1/4th order derivative of $g(t)$. By applying the Cauchy-Schwarz inequality twice we can instead get a bound in terms of standard derivatives,

$$\begin{aligned}
\|u_-(\cdot,t)\|^2 &= C\sqrt{\varepsilon} \int_{-\infty}^{\infty} |\xi|^{1/2} |\hat{g}(i\xi)|^2 d\xi \\
&\leq C\sqrt{\varepsilon} \left(\int_{-\infty}^{\infty} |\hat{g}(i\xi)|^2 d\xi \right)^{1/2} \left(\int_{-\infty}^{\infty} |\xi| |\hat{g}(i\xi)|^2 d\xi \right)^{1/2} \\
&\leq C\sqrt{\varepsilon} \left(\int_{-\infty}^{\infty} |\hat{g}(i\xi)|^2 d\xi \right)^{3/4} \left(\int_{-\infty}^{\infty} |\xi|^2 |\hat{g}(i\xi)|^2 d\xi \right)^{1/4}. \tag{A.37}
\end{aligned}$$

We thereby get, by Parseval,

$$\|u_-(\cdot,t)\| \leq C\varepsilon^{1/4} \left(\int_{0}^{\infty} |g(t)|^2 dt \right)^{3/8} \left(\int_{0}^{\infty} |g'(t)|^2 dt \right)^{1/8}, \tag{A.38}$$

which can be rewritten as

$$\|u_-(\cdot,t)\| \le C\left(\int_0^\infty |g(t)|^2 \mathrm{d}t\right)^{1/2} + C\varepsilon\left(\int_0^\infty |g'(t)|^2 \mathrm{d}t\right)^{1/2}. \tag{A.39}$$

We bound the other term using its exponential decay in x, which is due to κ being non-positive

$$u_+(x,t) = \frac{1}{2\pi}\int_0^\infty \mathrm{e}^{\mathrm{i}\xi t}\mathrm{e}^{\kappa x}\hat{g}(\mathrm{i}\xi)\mathrm{d}\xi, \tag{A.40a}$$

$$\|u_+(\cdot,t)\|^2 = \int_0^\infty \left|\frac{1}{2\pi}\int_0^\infty \mathrm{e}^{\mathrm{i}\xi t}\mathrm{e}^{\kappa x}\hat{g}(\mathrm{i}\xi)\mathrm{d}\xi\right|^2 \mathrm{d}x. \tag{A.40b}$$

We have $\xi \ge 0$ and $\kappa = -\sqrt{2\xi/\varepsilon} \le 0$, with the inverse relation $\xi = \varepsilon\kappa^2/2$. We use this to substitute variables,

$$\begin{aligned}
\|u_+(\cdot,t)\|^2 &= \int_0^\infty \left|\frac{1}{2\pi}\int_0^{-\infty} \mathrm{e}^{\mathrm{i}\varepsilon\kappa^2 t/2}\mathrm{e}^{\kappa x}\hat{g}(\mathrm{i}\varepsilon\kappa^2/2)\varepsilon\kappa\mathrm{d}\kappa\right|^2 \mathrm{d}x \\
&\le C\int_0^\infty \int_{-\infty}^0 \left|\varepsilon\kappa\mathrm{e}^{\mathrm{i}\varepsilon\kappa^2 t/2}\mathrm{e}^{\kappa x}\hat{g}(\mathrm{i}\varepsilon\kappa^2/2)\right|^2 \mathrm{d}\kappa\mathrm{d}x.
\end{aligned} \tag{A.41}$$

By Lemma 3.1 of [3] the integral (A.41) converges. Changing the order of integration is therefore justified, and we get

$$\begin{aligned}
\|u_+(\cdot,t)\|^2 &\le C\int_{-\infty}^0 \left(\int_0^\infty \mathrm{e}^{2\kappa x}\mathrm{d}x\right)\varepsilon^2\kappa^2|\hat{g}(\mathrm{i}\varepsilon\kappa^2/2)|^2\mathrm{d}\kappa \\
&\le C\int_{-\infty}^0 -\varepsilon^2\frac{1}{2\kappa}\kappa^2|\hat{g}(\mathrm{i}\varepsilon\kappa^2/2)|^2\mathrm{d}\kappa \\
&\le C\int_0^\infty \varepsilon|\hat{g}(\mathrm{i}\xi)|^2\mathrm{d}\xi \\
&\le C\varepsilon\int_0^\infty |g(t)|^2\mathrm{d}t.
\end{aligned} \tag{A.42}$$

This contribution is negligible compared to the other, so the estimate is given by (A.39). By causality arguments, the boundary condition $g(t)$ for $t > T$ cannot affect the estimate. We can therefore truncate the integrals, yielding

$$\|u(\cdot,t)\| \le C\left(\int_0^T |g(t)|^2 \mathrm{d}t\right)^{1/2} + C\varepsilon\left(\int_0^T |g'(t)|^2 \mathrm{d}t\right)^{1/2}. \tag{A.43}$$

Finally, for the case with inhomogeneous initial condition,

$$u_t = \frac{\mathrm{i}\varepsilon}{2}u_{xx}, \quad u(0,t) = g(t), \quad u(x,0) = f(x), \tag{A.44}$$

we can decompose the solution as $u = v + w$, where v and w satisfies the subproblems

$$v_t = \frac{i\varepsilon}{2} v_{xx}, \qquad\qquad w_t = \frac{i\varepsilon}{2} w_{xx}, \qquad\qquad \text{(A.45a)}$$

$$v(0,t) = g(t), \qquad\qquad w(0,t) = 0, \qquad\qquad \text{(A.45b)}$$

$$v(x,0) = 0, \qquad\qquad w(x,0) = f(x). \qquad\qquad \text{(A.45c)}$$

Above we have derived an estimate for v, and w satisfies the standard energy estimate

$$\|w(\cdot,t)\| = \|f\| \quad \text{for all } t \geq 0. \qquad\qquad \text{(A.46)}$$

The desired result is given by the triangle inequality, $\|u\| \leq \|v\| + \|w\|$. So, the proof is completed. $\qquad\qquad\qquad\qquad\qquad\qquad\qquad\qquad\qquad\qquad\qquad\qquad\qquad\qquad \square$

References

[1] V. M. BABIČ AND V. S. BULDYREV, *Short-Wavelength Diffraction Theory: Asymptotic Methods*, Volume 4 of Springer Series on Wave Phenomena, Springer-Verlag, New York, NY, 1991.

[2] J.-P. BÉRENGER, *A perfectly matched layer for the absorption of electromagnetic waves*, J. Comput. Phys., 114 (1994), pp. 185–200.

[3] J. L. BONA, S. M. SUN, AND B.-Y. ZHANG, *A non-homogeneous boundary-value problem for the Korteweg-de Vries equation in a quarter plane*, Trans. Amer. Math. Soc., 354 (2002), pp. 427–490.

[4] M. H. CARPENTER, D. GOTTLIEB, AND S. ABARBANEL, *Time-stable boundary conditions for finite-difference schemes solving hyperbolic systems: Methodology and application to high-order compact schemes*, J. Comput. Phys., 111 (1994), pp. 220–236.

[5] V. ČERVENÝ, M. M. POPOV, AND I. PŠENČÍK, *Computation of wave fields in inhomogeneous media–Gaussian beam approach*, Geophys. J. R. Astr. Soc., 70 (1982), pp. 109–128.

[6] B. ENGQUIST AND O. RUNBORG, *Computational high frequency wave propagation*, Acta Numer., 12 (2003), pp. 181–266.

[7] G. A. HAGEDORN, *Raising and lowering operators for semiclassical wave packets*, Ann. Phys., 269 (1998), pp. 77–104.

[8] E. J. HELLER, *Time-dependent approach to semiclassical dynamics*, J. Chem. Phys., 62 (1975), pp. 1544–1555.

[9] N. R. HILL, *Gaussian beam migration*, Geophysics, 55 (1990), pp. 1416–1428.

[10] M. HOCHBRUCK, C. LUBICH, AND H. SELHOFER, *Exponential integrators for large systems of differential equations*, SIAM J. Sci. Comput., 19 (1998), pp. 1552–1574.

[11] M. HOCHBRUCK AND A. OSTERMANN, *Exponential Runge-Kutta methods for parabolic problems*, Appl. Numer. Math., 53 (2005), pp. 323–339.

[12] M. HOCHBRUCK AND A. OSTERMANN, *Exponential integrators*, Acta Numer., 19 (2010), pp. 209–286.

[13] S. JIN, P. MARKOWICH, AND C. SPARBER, *Mathematical and computational methods for semiclassical Schrödinger equations*, Acta Numer., 20 (2011), pp. 121–209.

[14] S. JIN AND P. QI, *A hybrid Schrödinger/ Gaussian beam solver for quantum barriers and surface hopping*, Kinet. Relat. Models, 4 (2011), pp. 1097–1120.

[15] J. B. KELLER, *Geometrical theory of diffraction*, J. Opt. Soc. Amer., 52 (1962), pp. 116–130.

[16] K. KORMANN, M. KRONBICHLER, AND B. MÜLLER, *Derivation of strictly stable high order difference approximations for variable-coefficient PDE*, J. Sci. Comput., 50 (2012), pp. 167–197.

[17] D. KOSLOFF AND R. KOSLOFF, *A Fourier method solution for the time dependent Schrödinger equation as a tool in molecular dynamics*, J. Comput. Phys., 52 (1983), pp. 35–53.

[18] H.-O. KREISS AND J. OLIGER, *Comparison of accurate methods for the integration of hyperbolic equations*, Tellus, 24 (1972), pp. 199–215.

[19] H.-O. KREISS AND G. SCHERER, *Finite element and finite difference methods for hyperbolic partial differential equations*, in Mathematical Aspects of Finite Elements in Partial Differential Equations, pages 195–212, New York, NY, 1974, Academic Press.

[20] H.-O. KREISS AND G. SCHERER, *On the existence of energy estimates for difference approximations for hyperbolic systems*, Technical report, Department of Computer Sciences, Uppsala University, 1977.

[21] H. LIU, O. RUNBORG, AND N. M. TANUSHEV, *Error estimates for Gaussian beam superpositions*, Math. Comput., 82 (2013), pp. 919–952.

[22] K. MATTSSON, *Summation by parts operators for finite difference approximations of second-derivatives with variable coefficients*, J. Sci. Comput., 51 (2012), pp. 650–682.

[23] K. MATTSSON AND J. NORDSTRÖM, *Summation by parts operators for finite difference approximations of second derivatives*, J. Comput. Phys., 199 (2004), pp. 503–540.

[24] M. MOTAMED AND O. RUNBORG, *Taylor expansion and discretization errors in Gaussian beam superposition*, Wave Motion, 47 (2010), pp. 421–439.

[25] A. NISSEN AND G. KREISS, *An optimized perfectly matched layer for the Schrödinger equation*, Commun. Comput. Phys., 9 (2011), pp. 147–179.

[26] A. NISSEN, G. KREISS, AND M. GERRITSEN, *High order stable finite difference methods for the Schrödinger equation*, J. Sci. Comput., 55 (2013), pp. 173–199.

[27] M. M. POPOV, *A new method of computation of wave fields using Gaussian beams*, Wave Motion, 4 (1982), pp. 85–97.

[28] J. RALSTON, *Gaussian beams and the propagation of singularities*, in Studies in Partial Differential Equations, Volume 23 of MAA Stud. Math., pages 206–248, Math. Assoc. America, Washington, D.C., 1982.

[29] A. TAFLOVE, Computational Electrodynamics: The Finite-Difference Time-Domain Method, Artech House, Boston, MA, 1995.

[30] D. J. TANNOR, Introduction to Quantum Mechanics: A Time-Dependent Perspective, University Science Books, Sausalito, CA, 2007.

[31] N. M. TANUSHEV, *Superpositions and higher order Gaussian beams*, Commun. Math. Sci., 6 (2008), pp. 449–475.

[32] N. M. TANUSHEV, Y.-H. R. TSAI, AND B. ENGQUIST, *A coupled finite difference–Gaussian beam method for high frequency wave propagation*, in B. Engquist, O. Runborg, and Y.-H. R. Tsai, editors, Numerical Analysis of Multiscale Computations, Volume 82 of Lecture Notes in Computational Science and Engineering, pages 401–420, Springer-Verlag, Berlin, 2012.